Chinese Chemical Letters 33 (2022) 4079–4083

Contents lists available at ScienceDirect

Chinese Chemical Letters

journal homepage: www.elsevier.com/locate/cclet

Green and controllable fabrication of nanocrystals from ionic liquids

Weizi Huang[a], Zhezheng Fang[a], Xianzi Zheng[a], Jianping Qi[a], Wei Wu[a,b,*], Yi Lu[a,*]

[a] Key Laboratory of Smart Drug Delivery of MOE, School of Pharmacy, Fudan University, Shanghai 201203, China
[b] Center for Medical Research and Innovation, Shanghai Pudong Hospital, Fudan University Pudong Medical Center, Shanghai 201399, China

ARTICLE INFO

Article history:
Received 28 June 2021
Revised 12 January 2022
Accepted 16 January 2022
Available online 22 January 2022

Keywords:
Nanocrystals
Ionic liquids
Bottom-up
Choline
Organic acids
Particle size

ABSTRACT

Nanocrystals are of great value in delivering poorly soluble drugs as a technique enables enhanced dissolution and bioavailability. The bottom-up technique allows better control of particle properties. However, the commonly used organic solvents are hazardous to environment and operators, and always lead to large particle size and wide size distribution due to failure on controlling the nucleation and crystal growth. The situation is exacerbated in scale-up production. Therefore, in the proof-of-concept study, we evaluated the feasibility of green and controllable fabrication of drug nanocrystals by using biocompatible ionic liquids (ILs) as solvents. Choline based ILs (Ch-ILs) were synthesized *via* metathesis reactions. Pure paclitaxel nanocrystals of high quality were obtained from Ch-ILs with surface tension higher than 42 mN/m. The sizes were below 250 nm, while the polydispersity indexes were lower than 0.25. Compared with ethanol, choline lactate is superior in controlling the size of the nanocrystals in scale-up production, where the drug concentration was increased by 6 times. The underlying mechanism may be due to the high viscosity and low surface tension of the ILs, which are supposed to benefit homogeneous and burst nucleation. Ch-ILs can be recycled from the process and recovery rate reached 91.1%. Moreover, the applicability of the green technique was validated in a wider range of model drugs and Ch-ILs. In conclusion, ILs are potent solvents in bottom-up technique for green and controllable fabrication of nanocrystals.

Nanocrystals are crystalline drug particles with sizes falling in the nanoscale range, which provide a universal solution for delivering poorly soluble drugs [1–3]. Controlling the particle size and size distribution of nanocrystals is full of challenges. The bottom-up method grows nanocrystals from solution. A burst nucleation and a slow growth of crystals are crucial to obtain uniform and high-quality nanocrystals [4,5]. It is ideal that nucleation is not triggered off during the mixing of solvent and anti-solvent until homogeneous mixture [6,7]. Otherwise, successive nucleation along the mixing progress of solvent and antisolvent streams leads to particles of different size and eventually, fewer and larger crystals (due to Ostwald's Ripening). The scale-up further exacerbates the situation.

Ionic liquids (ILs) are salts with melting points below 100 °C [8,9]. Due to the non-flammability, low volatility, high tailorability, and excellent solvability, ILs are well known green solvents substituting for conventional volatile organic compounds (VOCs) in chemical industry [10–12]. Albeit being good solvent for poorly soluble drugs, ILs lose the solubilizing capability upon mixing with water due to ionic dissociation. Thus, ILs and water can be adopted as solvent and anti-solvent, respectively, to prepare nanocrystals. ILs form aggregates, ion triplets, and contact pairs upon mixing with water [13]. The structures may keep solubilization of active pharmaceutical ingredients (APIs) till infinite dilution (complete dissociation to free ions). The viscous properties of ILs may delay the progress to infinite dilution, which is advantageous to alleviate successive nucleation during the mixing process. Therefore, the feasibility of using choline (Ch)-based ILs (Ch-ILs) as green alternatives to VOCs in nanocrystal fabrications is investigated.

Scheme 1 shows the process. Drugs are firstly dissolved in ILs. Upon introduction of water, the anti-solvent, into the solution, ILs lose the solubilizing capability due to ionic dissociation and lead to precipitation of the drug. The resulted nanocrystals are collected by filtration. The ILs are recovered by evaporating water from the ionic solution.

Organic acids used in the synthesis of Ch-ILs are all from natural sources and indexed in GRAS (generally recognized as safe) by FDA, including acetic acid (Ace), lactic acid (Lac), malonic acid (Mal), *n*-butyric acid (*n*-Bu), succinic acid (Suc), malic acid (Mala), *n*-hexanoic acid (*n*-Hx), and citric acid (Cit). Metathesis reaction was used to synthesize the ILs [14,15]. The obtained Ch-ILs were transparent and viscous liquids at room temperature (Fig. S1 in Supporting information). The structure and composition of Ch-ILs

* Corresponding authors.
E-mail addresses: wuwei@shmu.edu.cn (W. Wu), fd_luyi@fudan.edu.cn (Y. Lu).

https://doi.org/10.1016/j.cclet.2022.01.043
1001-8417/

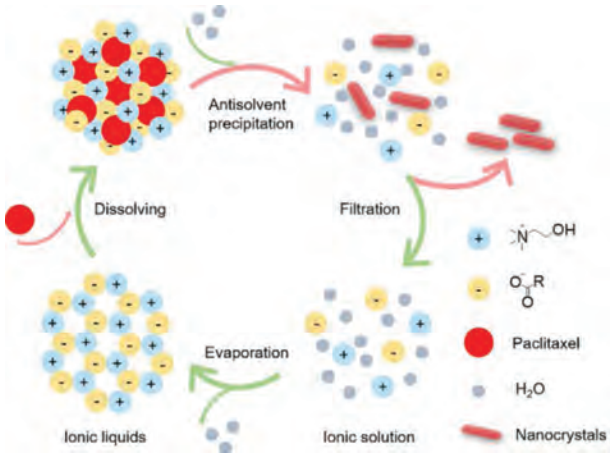

Scheme 1. Schematic diagram of the Ch-ILs based fabrication of nanocrystals.

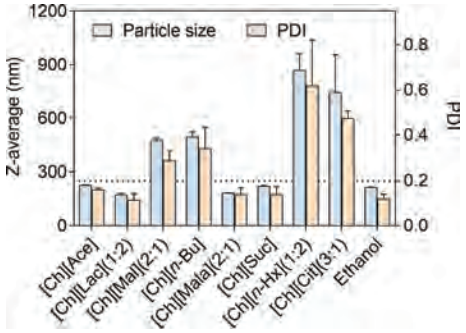

Fig. 1. Effect of Ch-ILs on particle size and PDI of PTX nanocrystals utilizing Ch-ILs and ethanol.

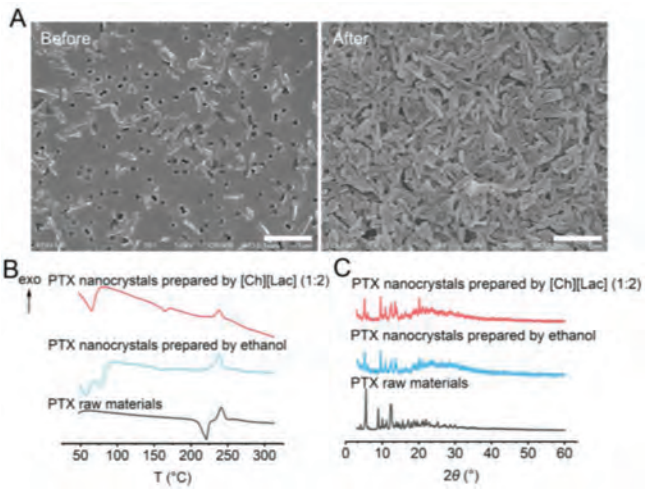

Fig. 2. Characterization of PTX nanocrystals. (A) Morphology before filtration and after resuspension. (B) Differential scanning calorimetry (DSC) patterns of PTX nanocrystals prepared from either [Ch][Lac] (1:2) or ethanol, and PTX raw materials. (C) Powder X-Ray diffraction (PXRD) patterns of PTX nanocrystals that are prepared from either [Ch][Lac] (1:2) or ethanol, and PTX raw materials. Scale bar: 1 μm.

were confirmed by proton nuclear magnetic resonance (^{1}H NMR) (Figs. S2-S9 in Supporting information). Table S1 (Supporting information) shows physicochemical properties of Ch-ILs. The viscosity of synthesized Ch-ILs varied from 38.9 mPa s to 2840.6 mPa s, being much higher than conventional VOCs; the surface tension ranged from 27.17 mN/m to 62.48 mN/m. It was obvious that the structure of anions had effects on physicochemical properties of Ch-ILs. Generally, increase in the chain length, number of polar substituents, and unsaturation could lead to the growth in viscosity of Ch-ILs. This might be due to the increased van der Waals or hydrogen bond interactions in ion network [16]. The surface tension decreased with the increase of the chain length, probably due to the reduced order and enriched nonpolar structure of surface composition [17].

Fig. 1 shows the size and polydispersity index (PDI) of prepared paclitaxel (PTX) nanocrystals. PDI value less than 0.25 is believed to be a uniform distribution of nanoparticles [18]. When ethanol was used as the solvent, the PTX nanocrystals presented the size of 250 nm with PDI value of 0.18. The composition of Ch-ILs affected the size and PDI of PTX nanocrystals. Due to the poor solubility in [Ch][Mal] (2:1) and [Ch][Cit] (3:1), *e.g.*, less than 1 mg/g, PTX tended to precipitate during the mixing process, leading to larger particle size and PDI than nanocrystals made from ethanol. Nanocrystals prepared from [Ch][Ace], [Ch][Lac] (1:2), [Ch][Mala] (2:1), and [Ch][Suc] were similar to that from ethanol, which were 150–300 nm in the average particle size with PDI value below 0.2 (Fig. 1). However, the size and PDI of PTX nanocrystals increased with the chain length of anions in ILs. Both the size and PDI increased to 496.8 ± 27.01 nm and 0.34 ± 0.01 for [Ch][*n*-Bu], and 869.0 ± 91.70 nm and 0.62 ± 0.20 for [Ch][*n*-Hx] (1:2), respectively (Fig. 1).

The direct change associated with the increase in chain length of fatty acids was reduced surface tension of corresponding ILs. It was generally acknowledged that low surface tension promoted nucleation according to the classical nucleation equation [7,19,20]. However, only the ILs with surface tension higher than 42 mN/m (*e.g.*, [Ch][Ace], [Ch][Lac] (1:2), [Ch][Mala] (2:1), and [Ch][Suc]) could lead to high quality PTX nanocrystals. As far as [Ch][*n*-Bu] and [Ch][*n*-Hx] (1:2) were concerned, although they presented even lower surface tension, the resulted PTX nanocrystals were larger. The reason might be due to molecular interactions between PTX and ILs. Surface tension decreased with the increase in log*P* of anions (Table S1 in Supporting information). Due to the hydrophobic interaction, PTX had stronger affinity to [Ch][*n*-Bu] and [Ch][*n*-Hx] (1:2). Nucleation of PTX during solvent/antisolvent mixing was thus retarded, leading to larger nanocrystals [20]. On the contrary, Ch-ILs with surface tension larger than 42 mN/m were composed of hydrophilic anions. Molecular interactions between PTX and these ILs were supposed to be weaker in comparison with [Ch][*n*-Bu] and [Ch][*n*-Hx] (1:2). In addition, the surface tensions of these Ch-ILs were lower than that of water (approximately 72 mN/m, 298.15 K) [21], which was advantageous to burst nucleation of PTX and consequently the control on size and size distribution of nanocrystals.

Viscosity is another important property affecting the bottom-up process. Unlike the surface tension, we did not find clear viscosity boundary to distinguish ILs that enable production of high quality PTX nanocrystals. However, all the ILs were far viscous than VOCs and water due to the continuous network formed by ions. The viscous network was not easily broken apart along invasion of water but was divided into smaller clusters [13,22]. We assume that the viscous ILs could be temporarily dispersed in water to form ultrafine droplets, which prevented the diffusion of PTX molecules from the ILs phase into the aqueous phase [20,23]. Following a thorough mixing, the ILs lost solubilizing capability due to dissociation of ion pairs, leading to instantaneous and synchronous nucleation of PTX. Consequently, small and uniform PTX nanocrystals were obtained.

Besides the surface tension and the viscosity, factors such as the concentration of the drug, volume ratio of ILs to water, the stirring speed during mixing, the temperature, and others may affect the size and size distribution of nanocrystals [20]. Since the purpose

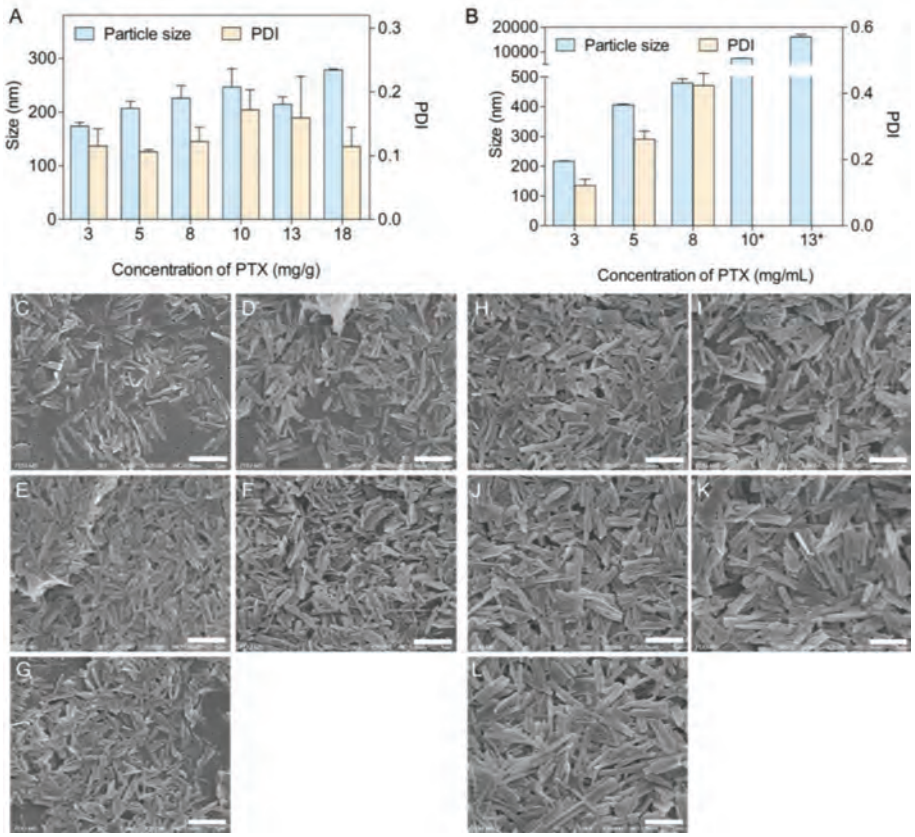

Fig. 3. DLS results of particle size and PDI of products prepared by (A) [Ch][Lac] (1:2) and (B) ethanol under different drug concentration (*, Dx50 value measured by Mastersizer 3000); SEM photographs of products prepared at drug concentration of (C) 5 mg/g, (D) 8 mg/g, (E) 10 mg/g, (F) 13 mg/g, and (G) 18 mg/g in [Ch][Lac] (1:2), and products prepared at drug concentration of (H) 3 mg/mL, (I) 5 mg/mL, (J) 8 mg/mL, (K) 10 mg/mL and (L) 13 mg/mL in ethanol, respectively. Scale bar: 1 μm.

of the study is to validate the feasibility of ILs in the preparation of nanocrystals, we didn't optimize these factors. The formula and process parameters were directly adopted from literature. The influence of these factors on the size should be investigated if the technique is applied to unknown drugs.

Based on the particle size and PDI, PTX nanocrystals prepared from [Ch][Lac] (1:2) were chosen for characterization. Fig. 2A shows SEM photographs of PTX nanocrystals before filtration and after resuspension. PTX nanocrystals were rod-shaped with uniform size distribution. The filtration was essential to remove the ions and concentrate the product. The process did not affect the quality of the PTX nanocrystals.

DSC patterns of PTX raw materials and two nanocrystals were shown in Fig. 2B. The endothermic peak at 220.8 °C of PTX raw materials referred to its melting point, which disappeared in the spectra of nanocrystals. Similar results were reported previously that thermodynamic behaviors of nanocrystals were size-dependent [6,24]. Specifically, the latent heat of fusion and melting temperature of nanoparticles decreased with the decrease of particle size. Such size dependence was ascribed to the structurally perturbed layer and excess Gibbs free energy at the particle surface [25]. Therefore, endothermic phenomena of PTX nanocrystals at the melting point was significantly weakened in comparison with bulk drugs. Exothermic peak around 240 °C referred to drug decomposition, which was similar for PTX raw materials and nanocrystals. Moreover, since crystallization occurred in water, PTX•$2H_2O$ instead of dehydrated PTX precipitation was obtained. Endothermic peaks below 100 °C in the DSC pattern of nanocrystals were due to dehydration. Another thermal event taking place at 164.6 °C revealed transition of dehydrated PTX from a crystalline into semicrystalline state [26].

PXRD patterns are shown in Fig. 2C, illustrating the crystallinity of the products. PTX raw materials showed 2θ peaks at 5.6°, 8.9°, 10.1°, 11.2°, 12.4°, 13.9°, 14.5°, 15.6°, 17.1°, 19.6°, and 22.0°, belonging to the dehydrated PTX crystals. Both two nanocrystals showed similar 2θ peaks at 5.2°, 6.1°, 9.6°, 10.9°, 12.2°, 12.4°, 13.6°, 13.9°, 15.3°, 16.4°, and 20.2°, belonging to PTX•$2H_2O$ [26]. Compared with ethanol, [Ch][Lac] (1:2) did not change the crystal form of PTX nanocrystals.

We tried to prepare nanocrystals at higher PTX concentration. The solubility of PTX in [Ch][Lac] (1:2) was measured to be 9.74 ± 0.64 mg/g at 25 °C and 18.13 ± 0.15 mg/g at 50 °C, respectively. Therefore, [Ch][Lac] (1:2) was heated to 50 °C to get PTX concentration larger than 10 mg/g, while 18 mg/g was set as the maximum concentration. Both the particle size and PDI of PTX nanocrystals slightly increased at higher PTX concentration in [Ch][Lac] (1:2), which were all below 300 nm and 0.20, respectively (Fig. 3A). Even when the concentration of PTX was close to the saturation solubility in [Ch][Lac] (1:2), uniform nanocrystals with size of 278.5 ± 1.504 nm can be prepared. SEM photographs (Figs. 3C-G) confirmed the results. On the contrary, when ethanol was adopted as the solvent, sharp increase on size and PDI of products was observed at higher PTX concentration (Figs. 3B and H-L). When PTX concentration exceeded 8 mg/mL in ethanol, the size of nanocrystals reached 479.0 ± 14.63 nm with PDI value as high as 0.424 ± 0.037. Further increase in concentration even led to PTX crystals of micrometers. Similar results were obtained when ethanol was adopted as the solvent in other bottom-up processes [27,28].

Although ILs were advantageous in controlling the size and size distribution of PTX nanocrystals, the batch size in technique screening was limited. Therefore, we studied the scale-up capabil-

ity of the technique. Firstly, the amount of each component was increased by 10 times or 20 times in proportion. The size and PDI values of PTX nanocrystals were not significantly increased comparing with the products in small batch (Table S2 in Supporting information). Then, at 20-fold level of magnification, we further increased the concentration of PTX in [Ch][Lac] (1:2) to 8 mg/g and 18 mg/g, respectively. Only slight increase in particle size and PDI value was found when the PTX concentration was increased to 18 mg/g (Table S2 in Supporting information), which were 301.9 ± 53.92 nm and 0.250 ± 0.069, respectively. The morphology of the PTX nanocrystals is shown in Fig. S10A (Supporting information). They were uniformly dispersed rod-like crystals with clear boundaries, indicating a high level of quality. The results also confirmed the strong capability of ILs in the bottom-up process to control the size of nanocrystals.

Due to the absence of stabilizers and the insolubility of PTX in water, it was rational to recycle ILs used in the technique. In addition, the adopted ILs consisted of hydrophilic ions. The ionic solution could be completely separated from PTX nanocrystals by filtration. Then removal of water *via* evaporation enabled recovery of ILs. The maximum recovery of [Ch][Lac] (1:2) was 91.1%, while the average recovery amounted to 81.9% in 3 consecutive cycles (Table S3 in Supporting information). Fig. S10B (Supporting information) shows the ^{1}H NMR spectrum of the recycled [Ch][Lac] (1:2), which was coincident with the fresh one. Neither deviation of proton chemical shifts nor additional sharp signals was observed, indicating no residuals of PTX [29]. The ratio of lactate to choline in recycled solvent (1.7:1) was similar to that of the fresh one (1.8:1). However, a broad peak emerged at around 4.75 ppm, which could be ascribed to signals of active hydrogens in choline and lactate. We evaluated the size and PDI of PTX nanocrystals prepared from the recycled [Ch][Lac] (1:2). The size was all below 250 nm, while the PDI values was less than 0.2 (Table S3 in Supporting information). The results further supported the green conception of the technique.

The applicability of the technique was validated in a wider range of model drugs and using [Ch][Ace] as a model Ch-ILs. [Ch][Ace] did not change the size and PDI of the nanosuspensions, being similar to that from the VOCs (Table S4 in Supporting information). Of note is that we did not optimize the preparation process, instead, the VOCs were directly substituted by an equal amount of [Ch][Ace]. [Ch][Ace] did not change the morphology of the nanosuspensions (Fig. 4), although different morphologies of nanosuspensions were obtained. The reason is due to the specific crystal habit of the individual API. Moreover, the solid-states were the same for the nanosuspensions prepared from [Ch][Ace] and VOCs (Figs. S11-S13 in Supporting information). Confirmed by DSC and PXRD evaluation, simvastatin and quercetin maintained the crystalline nature following antisolvent precipitation, but ursodeoxycholic acid was transformed to amorphous.

In conclusion, a series of Ch-ILs with different properties were synthesized by metathesis reactions. Ch-ILs with surface tension larger than 42 mN/m could be adopted as solvents to prepare pure PTX nanocrystals of high quality by using a bottom-up approach. PTX nanocrystals with size below 250 nm and PDI less than 0.25 were obtained. The nanocrystals made from [Ch][Lac] (1:2) were similar to that from ethanol in size, PDI, and solid-state properties. [Ch][Lac] (1:2) seemed to be superior to ethanol in controlling the size of PTX nanocrystals in scale-up production. The underlying mechanism was probably related to the high viscosity of ILs to prevent inhomogeneous nucleation as well as the low surface tension to promote nucleation. Moreover, [Ch][Lac] (1:2) could be recovered for cyclic utilization without compromise on the quality of PTX nanocrystals. Besides PTX and [Ch][Lac] (1:2), nanosuspensions of a wider range of model drugs have also been obtained from [Ch][Ace], indicating a good applicability of the technique. In conclusion, ILs are likely to be a potent solution for green and controllable fabrication of drug nanocrystals.

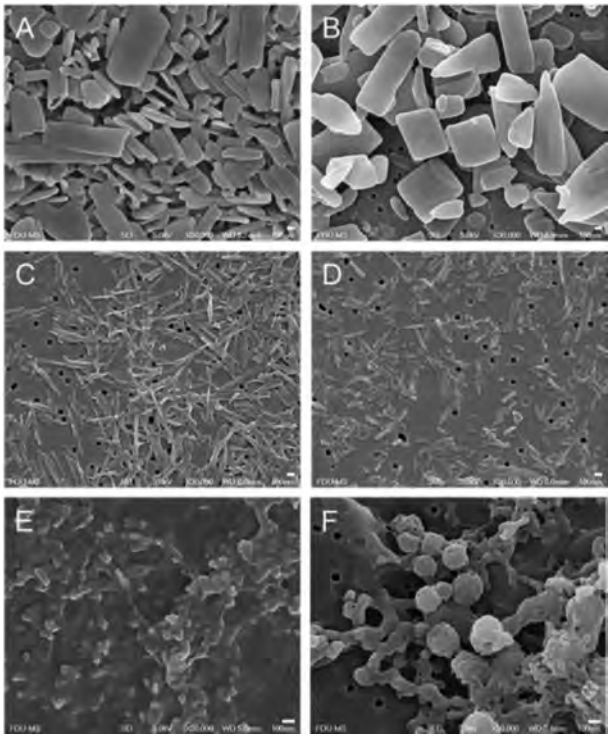

Fig. 4. Morphologies of simvastatin nanosuspensions prepared from (A) methanol and (B) [Ch][Ace], quercetin nanosuspensions prepared from (C) ethanol and (D) [Ch][Ace], ursodeoxycholic acid nanosuspensions prepared through (E) alkali-acid neutralization and from (F) [Ch][Ace]. Scale bar: 100 nm.

Declaration of competing interest

The authors declare that they have no known competing financial interests or personal relationships that could have appeared to influence the work reported in this paper.

Acknowledgments

This work was supported by the National Natural Science Foundation of China (Nos. 82030107 and 81973247), and Science and Technology Commission of Shanghai Municipality (Nos. 19XD1400300, 19430741400, 19410761200).

Supplementary materials

Supplementary material associated with this article can be found, in the online version, at doi:10.1016/j.cclet.2022.01.043.

References

[1] Z.J. Chen, W. Wu, Y. Lu, Ther. Deliv. 11 (2020) 225–230.
[2] Y. Lu, Y. Lv, T. Li, Adv. Drug Deliv. Rev. 143 (2019) 115–133.
[3] Y. Li, C. Teng, H.S. Azevedo, L. Yin, W. He, Chin. Chem. Lett. 32 (2021) 3071–3075.
[4] S.M. D'Addio, R.K. Prud'homme, Adv. Drug Deliv. Rev. 63 (2011) 417–426.
[5] C. Teh, P.N. Manghnani, G.N.H. Boon, et al., Adv. Funct. Mater. 29 (2019) 1901226.
[6] X.T. Ren, J.P. Qi, W. Wu, et al., Acta Pharm. Sin. B 9 (2019) 118–127.
[7] S.G. Kwon, T. Hyeon, Small 7 (2011) 2685–2702.
[8] K.S. Egorova, E.G. Gordeev, V.P. Ananikov, Chem. Rev. 117 (2017) 7132–7189.
[9] W. Huang, X. Wu, J. Qi, et al., Drug Discov. Today 25 (2020) 901–908.
[10] S. Wegner, C. Janiak, Top. Curr. Chem. 375 (2017) 65.
[11] T.S. de Almeida, A. Júlio, J.P. Mota, P. Rijo, C.P. Reis, Ther. Deliv. 8 (2017) 461–473.

[12] S. Zhang, B. Cheng, Y. Fang, et al., Chin. Chem. Lett. (2021), doi:10.1016/j.cclet.2021.11.024.
[13] O. Nordness, J.F. Brennecke, Chem. Rev. 120 (2020) 12873–12902.
[14] X. Wu, H. Zhang, S. He, et al., Int. J. Biol. Macromol. 150 (2020) 528–535.
[15] E.E.L. Tanner, A.M. Curreri, J.P.R. Balkaran, et al., Adv. Mater. 31 (2019) e1901103.
[16] J.G. Huddleston, A.E. Visser, W.M. Reichert, et al., Green Chem. 3 (2001) 156–164.
[17] Z.C. Chen, O. Morales-Collazo, J.F. Brennecke, Langmuir 36 (2020) 8904–8913.
[18] Y. Xie, Z. Chen, R. Su, et al., Curr. Drug. Deliv. 14 (2017) 483–491.
[19] S.V. Dalvi, R.N. Dave, Ind. Eng. Chem. Res. 48 (2009) 7581–7593.
[20] B. Sinha, R.H. Muller, J.P. Moschwitzer, Int. J. Pharm. 453 (2013) 126–141.
[21] G.J. Gittens, J. Colloid Interface Sci. 30 (1969) 406–412.
[22] A.A. Padua, M.F. Costa Gomes, J.N. Canongia Lopes, Acc. Chem. Res. 40 (2007) 1087–1096.
[23] C. Beck, S.V. Dalvi, R.N. Dave, Chem. Eng. Sci. 65 (2010) 5669–5675.
[24] M. Fathollahi, S.M. Pourmortazavi, S.G. Hosseini, J. Energ. Mater. 26 (2007) 52–69.
[25] F. Delogu, J. Phys. Chem. B 109 (2005) 21938–21941.
[26] R.T. Liggins, W.L. Hunter, H.M. Burt, J. Pharm. Sci. 86 (1997) 1458–1463.
[27] Y. Lu, Z.H. Wang, T.L. Li, et al., J. Control. Release 176 (2014) 76–85.
[28] M. Kakran, N.G. Sahoo, I.L. Tan, L. Li, J. Nanopart. Res. 14 (2012) 757.
[29] Y. Zhang, Z. Guo, Z. Cao, et al., Biomaterials 183 (2018) 243–257.